第14回性能に基づく橋梁等の耐震設計に関する
シンポジウム講演論文集（2011年7月）

SEISMIC PERFORMANCE OF UFC JACKET PIERS

Rui Zhang[1], Tomohiro Sasaki[2], Mohamed. A. ElGawady [3], Kazuhiko Kawashima [4] and Hiroshi Matsuzaki[5]

[1]Department of Civil Engineering, Tokyo Institute of Technology, 2-12-1, O-Okayama, Meguro, Tokyo 152-8552, Japan
[2]Member, Hyogo Earthquake Engineering Research Center, National Research Institute for Earth Science and Disaster Prevention, Miki, Hyogo, 673-0515, Japan
[3] Department of Civil Engineering, Tokyo Institute of Technology, 2-12-1, O-Okayama, Meguro-ku, Tokyo 152-8552, Japan
[4] Fellow, Department of Civil Engineering, Tokyo Institute of Technology, 2-12-1, O-Okayama, Meguro, Tokyo 152-8552, Japan
[5] Member, Department of Civil Engineering, Tokyo Institute of Technology, 2-12-1, O-Okayama, Meguro, Tokyo 152-8552, Japan

1. Introduction

It was always observed in the past earthquakes that damage in reinforced concrete bridge columns occurred at the column base. Although different types of failure of bridge columns were observed, the sequence of damage is similar for those columns. The most notable observations, in sequence of occurrence, were cracking of cover concrete, yielding of longitudinal bars, spalling of cover concrete, fracture of tie bars, buckling of longitudinal reinforcements and fracture of longitudinal reinforcements. It indicates that delaying or preventing the compression failure of the cover concrete may result in enhancing the ductility capacity of a column. Therefore, the idea of implementation of concrete with extremely high compressive strength at the plastic hinge of column was brought out. It was proposed by Yamanabe et al. (2008) to replace the conventional concrete at the plastic hinge with ultra-high-performance steel-fiber-reinforced concrete (hereafter referred to as "UFC) which is one of innovative materials with highly advanced mechanical properties, superior physical characteristics and unprecedented ductility.

In 2009, two reinforced concrete columns UFC-1 and UFC-2 using UFC at the column base were constructed to clarify their seismic performance by Huang, S. et al. The specimen configuration and details are shown in **Fig. 1.** In both columns, UFC precast jackets were set at the column base to replace cover concrete. Brass mesh was set between UFC jackets in both columns as a crack-inducing mechanism so that plastic hinge mechanism can be formed in the core concrete.

Both columns were subjected to bilateral loading based on displacement control under a constant axial load of 160kN. Circular orbit was used for bilateral loading displacement with an increment of 0.5% drift until columns failed. Although the brass mesh was set to facilitate opening between UFC jackets, most joints between UFC jackets did not open during the experiments. Failure occurred at the footing rather than the expected region with UFC jackets.

Having learned from the lessons of the previous research, two types of columns using UFC precast jackets were proposed. Type I, RC-UFC column, is a conventional reinforced concrete column using UFC precast jackets at the plastic hinge. Type II, PC-UFC column, is a hollow column using UFC precast jackets with post-tension. Type I column (RC-UFC) is a modified version of a column by Wang *et al.* In Wang's model, separations between UFC jackets were not constrained and outer layer of longitudinal bars were unbonded in UFC jackets to make separations open more freely after being deformed. However, the interaction between UFC jackets and core concrete were not taken into consideration with the assumption that a plane of UFC and RC remains as a plane after deformation. In this study, the interaction between these two materials was clarified by employing interface elements at the interface between UFC jackets and RC section. To effectively utilize the ultra strength of UFC, another conceptual column, Type II column (PC-UFC) was proposed.

In this study, the seismic performance of the RC-UFC and PC-UFC under the loading conditions of pushover and hybrid loadings was clarified based on fiber element analysis.

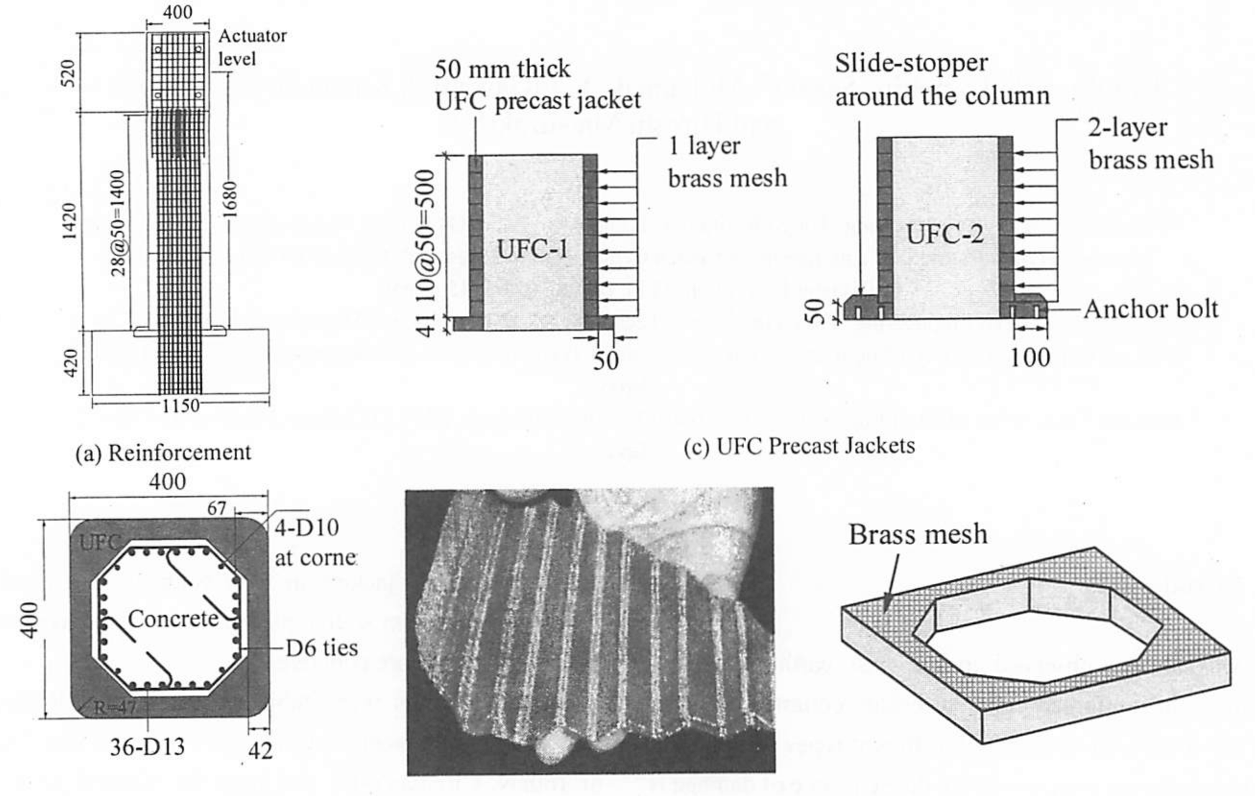

Fig. 1 Specimen configuration and details (Huang, S., 2010)

2. Design of UFC Jacket Piers

Both columns were scaled down by the geometrical scale of 6/35. The materials used in both columns are precast UFC segments, conventional concrete and steel bars. From the lesson learned from Huang's experiment, the surface of footing was designed to be UFC to prevent extensive damage. The longitudinal reinforcements were designed to be continuous from the footing to the column top, while it was unbonded from UFC segments in the UFC section but bonded with conventional RC in RC section.

Concrete with design strength of 27MPa was used in footing and the section above the footing. The steel bars used are SD345 with diameter 6mm. SD295 steel bar with diameter 4mm was used for tie bars. From 100mm below the footing surface to 600mm above the footing surface, UFC precast segments were set bonding with the conventional RC inside. The material properties are shown in **Table 1**. The configuration and dimensions of RC-UFC and PC-UFC columns are shown in **Fig. 2**.

Table 1 Material properties

Material	Standard	Elastic Modulus (MPa)
UFC	-	45,000
Concrete	C27	26,500
Longitudinal Bars	SD345-D6	200,000

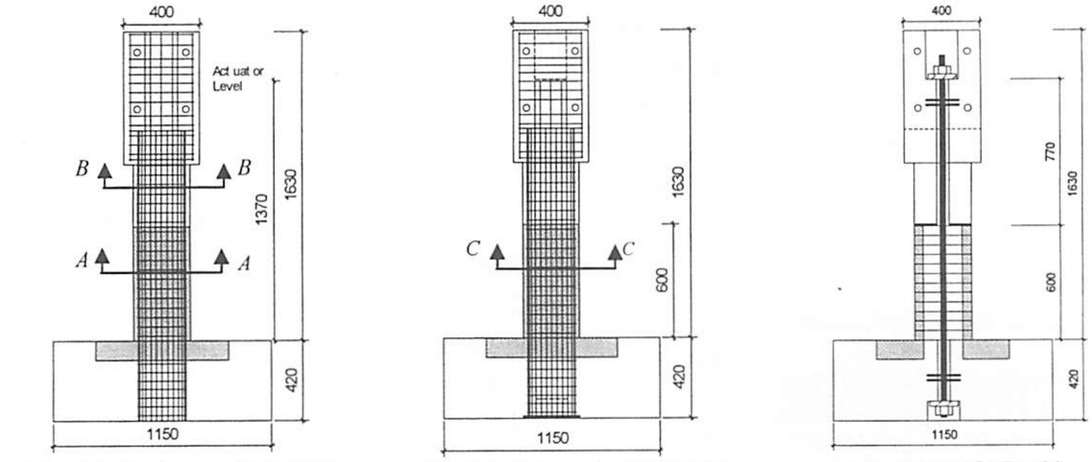

(a) Reinforcement of RC-UFC (b) Reinforcement of PC-UFC (c) Setup of PC cable

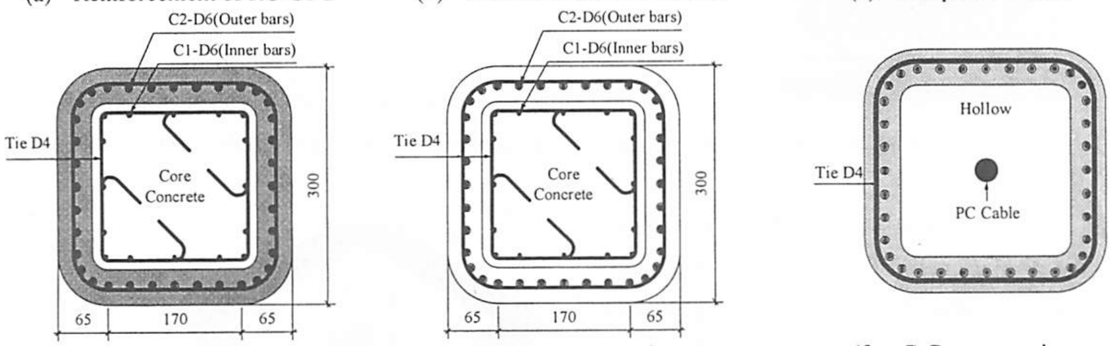

(d) A-A cross section (e) B-B cross section (f) C-C cross section

Fig. 2 Configuration and dimensions of RC-UFC and PC-UFC columns (unit: mm)

3. Modeling and Idealizations

Fiber element analysis is a developed numerical approach for structural nonlinear analysis. In this study, the element was subdivided into longitudinal fibers as shown in **Fig. 3**. In both columns, only the longitudinal steel bars bonded with concrete were modeled as fiber elements. The unbonded longitudinal steel bars penetrating UFC segments were idealized as truss elements. The purpose of setting these reinforcements is to make the separations between UFC jackets open more freely. Moreover, the unbonded bars were designed to increase the capacity of dissipating energy in the columns.

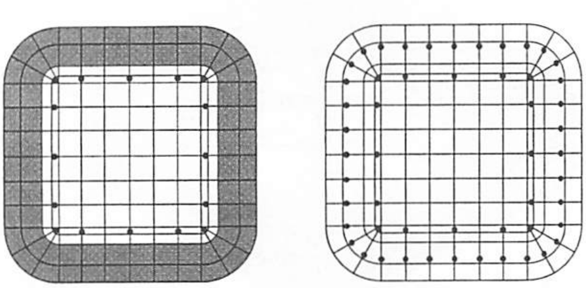

(a) A-A cross section (b) B-B cross section

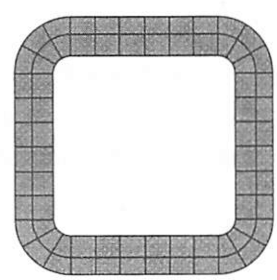

(c) C-C cross section

Fig. 3 Section Discretization

Based on the basic assumption that plane sections remain plane and normal to the longitudinal axis in fiber element analysis, all fiber strains and stresses act parallel to this axis. Since the reference axis is fixed, this indicates that the geometric centroids of the sections form a straight line that coincides with the reference axis. In this study, central nodes which represent centroids of sections were modeled differently due to the absence of core concrete in UFC jackets in PC-UFC model.

In RC-UFC model, from the column base to the top of UFC section, 2 sets of nodes were modeled; RC nodes which simulate the RC core in the UFC segments, and UFC nodes which are to simulate the opening between UFC jackets. As shown in **Fig. 4**, central nodes of RC and UFC section are at the same location. The RC nodes were linked by RC fiber elements continuously from the footing until the beam elements at the top. Since the UFC precast segments are separated with each other, two central nodes which represent the centroids of the *i+1 th* and the *i th* UFC segmental lower and top plane, respectively.

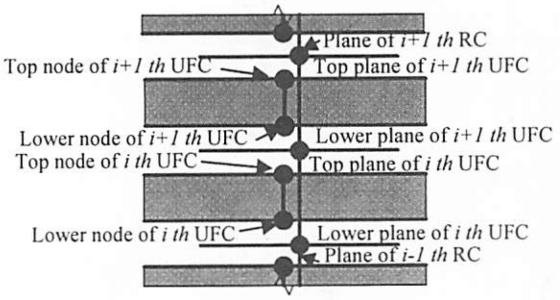

Fig. 4 Central nodes of RC and UFC section in RC-UFC model

The element deformations consist of three components; the displacement of RC and UFC segments and the interaction between them, which produces displacement compatibility. The transverse displacement perpendicular to the column axis is the same for concrete and UFC segments but vertical relative slipping between the two components produces a bond effect at the interface. The displacement of two adjacent points in the concrete core and UFC segments are calculated based on the axial and flexural deformation of their axis:

$$d_u = \bar{d}_u - w \cdot \theta_u \quad (1a)$$

$$d_c = \bar{d}_c - w \cdot \theta_c \quad (1b)$$

in which, d is deformation of plane, w is width of column; $\bar{d}$ and θ are the axial and rotational deformation of axis. The subscripts u and c are their values for UFC segments and concrete, respectively. The displacements of UFC segment and concrete are shown in **Fig. 5**.

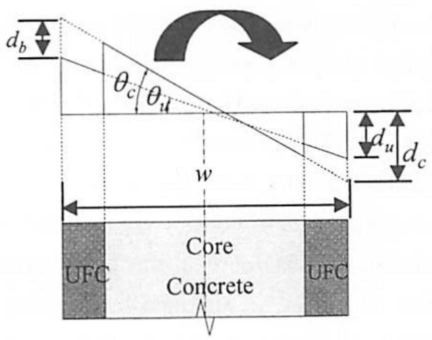

Fig. 5 Kinematics of RC-UFC Sections

The difference between two displacements cause the slipping as

$$d_b = \bar{d}_c - \bar{d}_u - w(\theta_c - \theta_u) \quad (1c)$$

For the purpose of evaluating the slipping between UFC jackets and concrete, the spring elements which are used to model the interface interaction were arranged along the interface on the top plane of UFC segments. The idealization of linking of UFC segments and RC section is shown in **Fig. 6**. Since the torsion was neglected in this analysis, the central node of UFC segments were linked to the one of RC section with rigid 'zero-length' tensional springs. Also, the lateral displacement between concrete core and UFC segment was constrained by 'zero-length' spring horizontally.

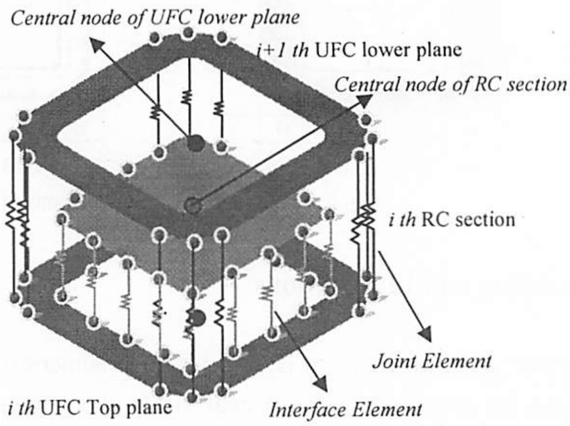

Fig. 6 Setup of interface elements and joint elements

The coordinates of two nodes linked by joint element which is called 'zero-length' spring are the same. The joint elements were idealized by nonlinear spring elements which do not take any tension force but with excessively large compressive stiffness.

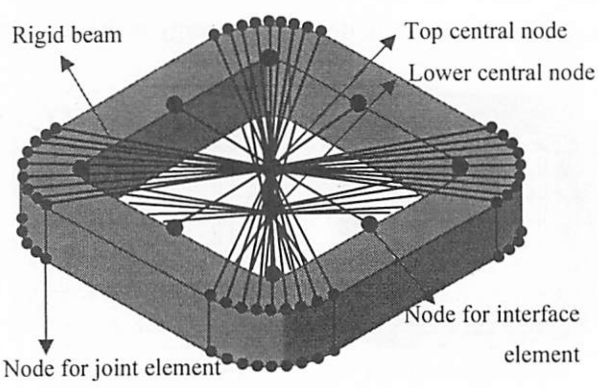

(a) UFC element

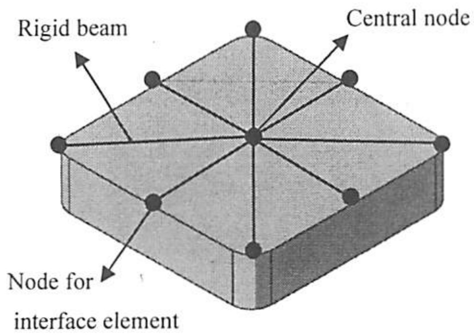

(b) RC element

Fig. 7 Nodes for Joints and Interface Elements

The interface elements were also modeled by 'zero-length' springs with nonlinear property. Two sets of nodes with the same coordinates were linked with RC and UFC central node by rigid beam, respectively, as shown in **Fig. 7**. The nonlinear properties of joint elements and interface elements are shown as **Fig. 8**. In PC-UFC column, since the UFC section is hollow, the interface elements were not employed, but the joint elements were the same as that used in RC-UFC column.

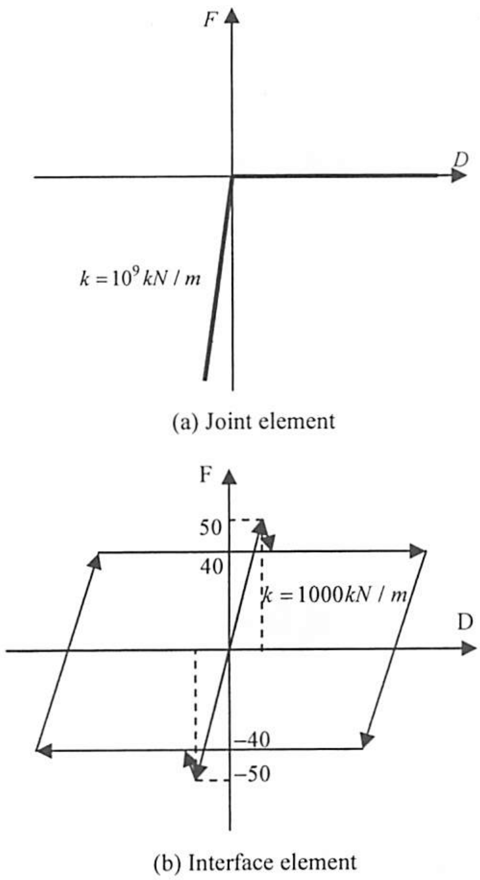

Fig. 8 Nonlinear properties of joint and interface element

In this study, the stress-strain hysteresis of concrete used is based on the work by Hoshikuma and Kawashima et al (1997). Unloading and reloading hysteresis used are idealized based on a model by Sakai and Kawashima (2000). The longitudinal reinforcement was idealized by the modified Menegotto-Pinto model which takes account of Bauschinger effect (Menegotto and Pinto 1973, Sakai and Kawashima 2003).

4 Evaluation of Ductility Capacity based on Pushover Analysis

Unilateral pushover analysis was conducted assuming a displacement increment of 0.137mm at the effective height of 1370mm from the column base. The analytical results of both columns are presented in **Fig. 9**.

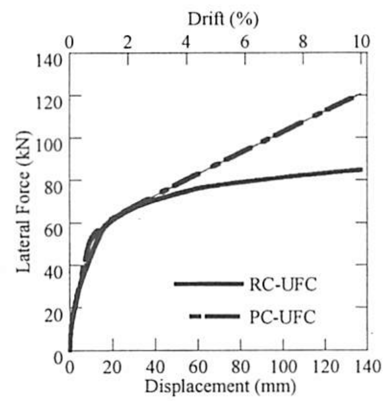

Fig. 9 Force-displacement relation at loading point

It is obvious that the lateral force of PC-UFC is 30% larger than that of RC-UFC at 10% drift. It should be noted that slipping between UFC jackets and core concrete occurred. The vertical relative displacement at the lowest UFC jacket is shown as **Fig. 10**. At the 6% drift, the dislocation of RC plane and UFC plane is shown in **Fig. 11**.

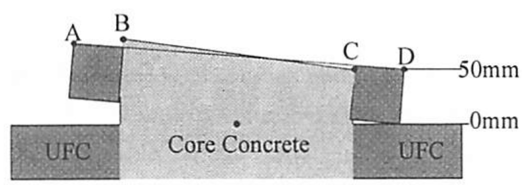

Fig. 10 Dislocation of RC Plane and UFC Segment at Top Plane

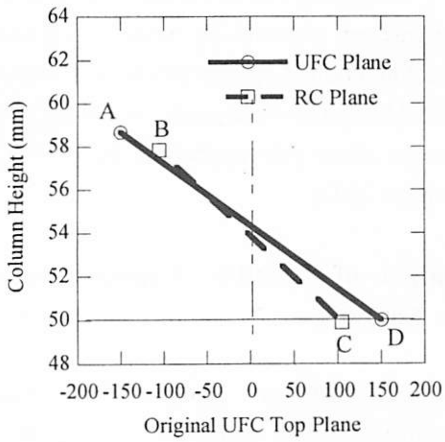

Fig. 11 Slipping at the lowest UFC jacket at 6% drift

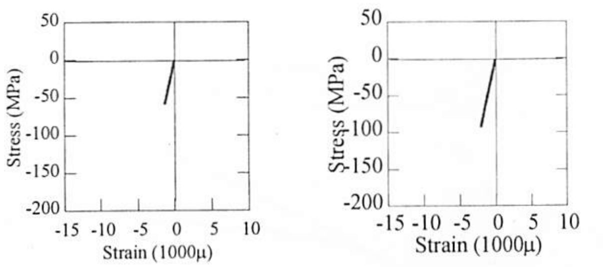

(a) RC-UFC (b) PC-UFC

Fig. 12 Stress-strain hysteresis of extreme compression fiber at 25mm level (10% drift)

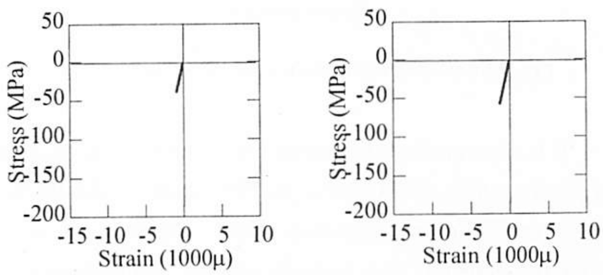

(a) RC-UFC (b) PC-UFC

Fig. 13 Stress-strain hysteresis of extreme compression fiber at 575mm level (10% drift)

Several possible vulnerable locations, such as column base and connection between RC section and UFC section, need to be examined. As shown in **Fig. 12, 13** and **14**, the stress-strain hysteresis of extreme compressive fiber at 10% drift indicates that no compression failure occurred at above mentioned locations in both columns. Meanwhile, the outmost longitudinal reinforcing bars on tensile side at above mentioned locations yielded as shown in **Fig. 15**. The opening between UFC jackets in both columns at 10% drift is shown in **Fig. 16.** The main openings of RC-UFC occurred from the column base to the height of 100mm and the connection between RC section and UFC section. Compared with RC-UFC, the main opening of PC-UFC concentrated only at the column base.

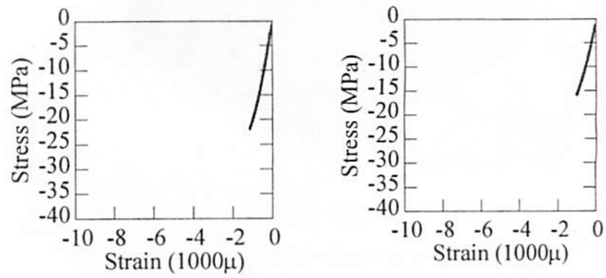

(a) RC-UFC (b) PC-UFC

Fig. 14 Stress-strain hysteresis of RC cover at extreme compression fiber at 625mm level (10% drift)

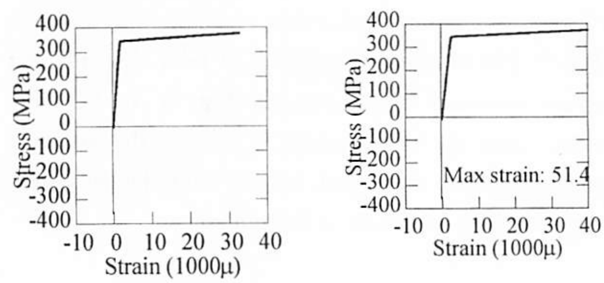

(a) RC-UFC (b) PC-UFC

Fig. 15 Stress-strain hysteresis of unbonded bars (10% drift)

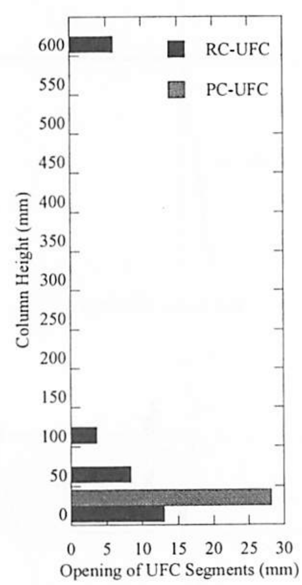

Fig. 16 Opening between UFC segments in two columns at 10% drift

5 Evaluation of Ductility Capacity Based on Hybrid Loading Analysis

NS and EW components of the ground avcceleration recorded at JR Takatori Station during the 1995 Kobe earthquake were used as input ground motion, which is shown in **Fig. 17**. The dominant period is 1~2s; the spectrum amplitude around the dominant period is about 4 (m/s). A constant vertical force of 86.1kN was applied at the top of column.

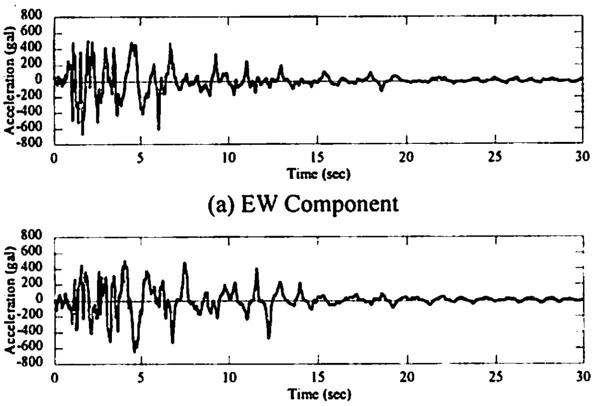

(b) NS Component

Fig. 17 JR Takatori Station Ground Motion Recorded during 1995 Kobe Earthquake

Since the SW direction is the direction with the largest response, the extreme fiber in SW direction at above mentioned possible vulnerable locations were examined. The response displacement of the two columns under the 100% NS and EW Takatori ground motions is shown in **Fig. 18**. It shows that the response displacement of PC-UFC is larger than that of RC-UFC. The stress-strain hysteresis of extreme fiber at SW direction is shown in **Fig. 19**, which indicates that the stress of PC-UFC is greater than that of RC-UFC. Nevertheless, the peak stresses did not reach the compression strength of UFC in the two columns, which indicates that the compression failure at the column base was prevented by using UFC jackets. As shown in **Fig. 20** and **Fig. 21**, the UFC cover in SW direction is still in the elastic range, but the RC cover at 625mm level suffered slight damage in terms of cracking.

In RC-UFC and PC-UFC columns, the unbonded longitudinal bars in SW direction were examined. As shown in **Fig. 22**, the unbonded bars yielded but the peak strains in both columns are much smaller than the rupture strain of 20%. It should be noted that the peak strain of PC-UFC column is almost 2 times than that of RC-UFC.

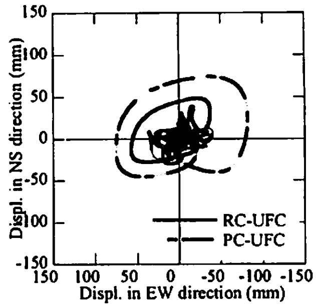

Fig. 18 Response displacement at loading point

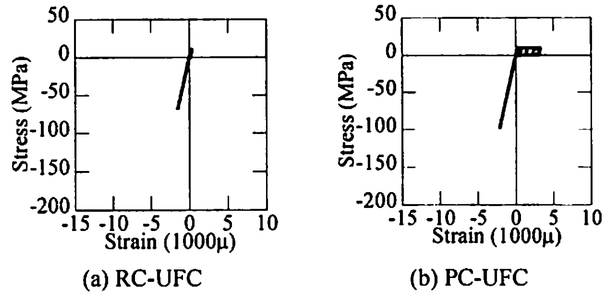

Fig. 19 Stress vs. Strain of UFC Cover at 25mm from the Base

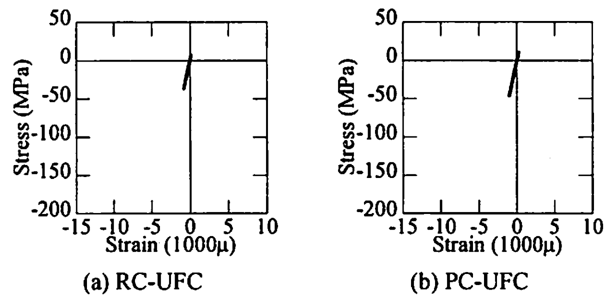

Fig. 20 Stress vs. Strain of UFC Cover at 575mm from the Base

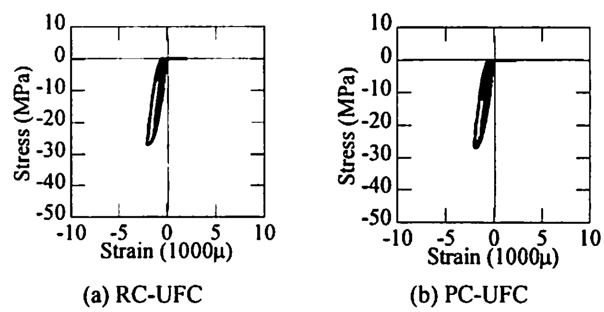

Fig. 21 Stress vs. Strain of RC Cover at 625mm level

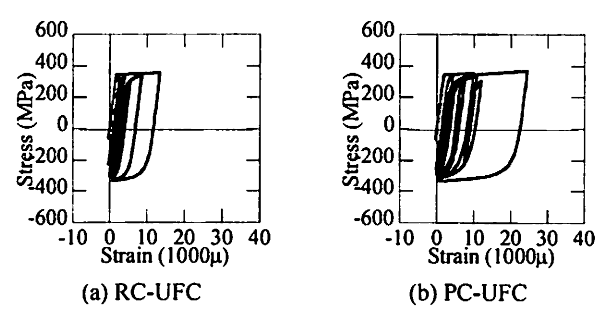

Fig. 22 Stress vs. Strain of unbonded bar in SW direction

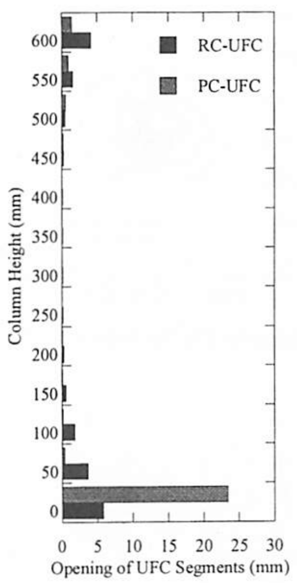

Fig. 23 Maximum separation between UFC Segments in two columns

The maximum separations in both columns are shown in **Fig. 23**. The openings of RC-UFC mainly concentrated in the region from the column base to 100mm from the base and connection between RC section and UFC section. However, the openings in PC-UFC mainly concentrated at the column base.

5 Conclusions

The use of ultra-high-performance steel-fiber - reinforced concrete can enhance the seismic performance of bridge columns. Based on the results presented, the following conclusions were deduced.

a) The cover concrete crushing was prevented with the use of UFC because of its high compressive strength.

b) In the UFC-RC column, the interaction between UFC segments and core concrete influences the performance of bridge column significantly. The performance of bridge column will be overestimated if the interaction between these two materials is ignored.

c) To further exploit the strength of UFC, applying post tension such as in the PC-UFC column investigated here, can further enhance the seismic performance of column compared with the RC-UFC column. On the other hand, openings at separations will be concentrated at the column base.

References

1) Yamanobe, S., Sogabe, N., Iemura H. and Takahashi, Y.: Development of High-Seismic- Performance Reinforced Concrete Bridge Pier with High-Performance Plastic Hinge, Proc. JSCE, Vol. 64, No. 2, pp. 317-332, 2008.

2) Huang, S.: Experimental Study on Seismic Performance of Columns Using Ultra-High-Strength Steel-Fiber-Reinforced Concrete Jackets, Master Thesis, Department of Civil engineering, Tokyo Institute of Technology, 2010.

3) Bache, H. H.: Introduction to Compact Reinforced Composite, Nordic Concrete Research, Vol. 6, pp.19-33, 1987.

4) Hoshikuma, J., Kawashima, K., Nagaya, K. and Taylor, A.W: Stress-Strain Model for Confined Reinforced Concrete in Bridges Pier, Journal of Structural Engineering, ASCE, Vol. 123, No. 5, pp. 624-633, 1997

5) Sakai, J. and Kawashima, K.: Unloading and Reloading Stress-Strain Model for Confined Concrete, Journal of Structural Engineering, ASCE, Vol. 132, No. 1, pp. 112-122, 2006.

6) Hayakawa, R. and Kawashima, K : Three-Dimensional Modeling of Reinforced Concrete with Multi-Directional Cracking, Concrete Library, JSCE, No. 36, pp. 181-206, 2000.